RSC Advances

ROYAL SOCIETY OF CHEMISTRY

www.rsc.org/advances

Recent Advances in Thermoelectric Materials and Solar Thermoelectric Generators – A Critical Review

Pradeepkumar Sundarraj[a], Dipak Maity[a], Susanta Sinha Roy[b] and Robert A Taylor[c]

[a]*Department of Mechanical Engineering, School of Engineering, Shiv Nadar University, India -203207*

[b]*Department of Physics, School of Natural Science, Shiv Nadar University, India - 203207*

[c]*School of Mechanical and Manufacturing Engineering and School of Photovoltaic and Renewable Energy Engineering, University of New South Wales, Australia*

Corresponding author:

Dipak Maity (Tel: +91-120-663801, and E-mail: dipakmaity@snu.edu.in)

Abstract

Due to the fact that much of the world's best solar resources are inversely correlated with population centers, significant motivation exists for developing the technology, which can deliver reliable and autonomous conversion of sunlight into electricity. Thermoelectric generators are gaining incremental ground in this area since they do not require moving parts and work well in remote locations. Thermoelectric materials have been extensively used in space satellites, automobiles, and, more recently, in solar thermal plants as power generators, known as solar thermoelectric generators (STEG). STEG systems are gaining significant interest in both, concentrated and non-concentrated systems and have been employed in hybrid configurations with the solar thermal and photovoltaic systems. In this article, the key developments in the field of thermoelectric materials and on-going research work on STEG design conducted by various researchers to date are critically reviewed. Finally, we highlight the strategic research directions to make highly efficient thermoelectric materials for developing the cost-effective STEG system, which could serve to bring this technology towards commercial readiness.

Keywords: Solar thermoelectric generator; Thermoelectric materials; Non-concentrating system; Concentrating system; Photovoltaic-TEG system, Thermal-TEG system

A. Introduction

The average global electric power consumption in 2011 was estimated at 17.4 terawatts,[1] but it is projected to be more than double and triple by 2050 and 2100, respectively.[2-4] At their present rate of use, *economically* recoverable fossil fuel resources will be severely depleted on these time scales (particularly if their full environmental cost is considered).[5-8] Hence, a major global challenge is how to meet future energy demand in a renewable and sustainable manner. Solar-derived electricity represents a vast, largely untapped renewable energy resource, which can be harvested through either photovoltaic or thermal routes.[5, 9] In this paper, we review the progress of one thermal route in particular, Solar Thermoelectric Generators (STEGs), which have recently been gaining research attention due to improvements in thermoelectric materials properties as well as in STEG system design. These improvements, if sustained, could eventually result in a new class of efficient, cost effective solar to electricity conversion systems.[8, 10]

A.1. ***Solar-to-electricity conversion technology***

The average solar radiation received on Earth is about 162,000 TW, whereas only a vanishingly small fraction of this power are diverted towards electricity generation.[1] Solar photovoltaic cells (PV) convert some of the solar spectrum directly into electricity,[11] while concentrated solar thermal (CST) technologies first convert incident solar energy to heat and then (usually) use this heat to boil a working fluid which drives a Rankine cycle.[4, 12] Various PV cells and CST system are compared in Table 1 with respect to their operational temperature, concentration ratio (CR = Area of the collector/Area of the receiver), and maximum efficiency. Laboratory scale PV modules have reached a maximum efficiency of about ~29% and a maximum efficiency of about 44% was attained for Concentrated photovoltaic (CPV) cell (Table 1).[13] However, commercially available solar PV modules, have efficiencies between 10-20%.[14] Commercially, large-scale CST projects have proven to be more efficient than PV cells.[15]

Solar thermal technologies use a structure (a collector) to receive and absorb solar thermal radiation; these collectors can be broadly classified into two types, non-concentrating and concentrating. Collectors, which do not concentrate sunlight, can be stationary and do not require tracking mechanisms. For most solar thermal electricity generation systems, however, concentration (and thus tracking) is required which adds to the system's capital cost. Another key component of the collector is the receiver – a heat exchanger that absorbs sunlight and transfers this energy as heat to a fluid passing through it.[7, 16, 17] Non-concentrating collectors are limited to a temperature range from ambient to 240 °C, while, depending on the CR, concentrating collectors (CST) can operate up to 1500 °C.[7]

Three prominent technologies dominate CST – parabolic trough collectors, solar towers, and dish systems.[4] Linear Fresnel system is rapidly emerging due to ease of manufacturing, operation and cost effectiveness,[18] which can achieve peak plant efficiency of about 18%.[15] Parabolic trough collectors have proven to be the most successful commercial solar thermal technology,[19] achieving a peak plant efficiency of about 20%.[15] Even though parabolic troughs and solar towers have their advantages on large scale, dish systems where a Stirling engine is placed at the receiver can achieve a maximum efficiency of about 30%. Solar Dish- Stirling (SDS) systems have garnered a lot of interest because they are well suited for decentralized power supply and stand-alone power applications.[15, 20, 21] However, more information about the long term performance of CPV and SDS may be required in order to commercialize these system.

Table 1. Efficiency and operating temperature of few solar energy conversion technologies [13, 15]

System	T °C	CR	η - max
I. Solar Photovoltaic (PV)			
Silicon (Si) crystalline	25	1	25.0±0.5
Gallium arsenide (GaAs) thin Film	25	1	28.8±0.9
Indium phosphide (InP) crystalline	25	1	22.1±0.7
Copper Indium Gallium Diselenide (CIS/ CIGS) cell	25	1	19.8±0.6
Cadmium Telluride (CdTe) cell	25	1	19.6±0.4
Dye-sensitized solar cell (DSSC)	25	1	11.9±0.4
Organic or Polymer (OPV) thin film	25	1	10.7±0.3
II. Concentrated Photovoltaic (CPV)			
Copper Indium Gallium Diselenide (CIS/ CIGS) thin film	-	15	22.8±0.9
Silicon (Si) single cell	-	92	27.6±1.0
Gallium arsenide (GaAs) single cell	-	117	29.1±1.3
InGaP/GaAs/InGaAs	-	302	44.4±2.6
III. Concentrated Solar Thermal (CST)			
Linear Fresnel Lens (LFL)	390	60-80	18
Parabolic Trough Collector (PTC)	350-550	70-80	20
Solar Tower (ST)	250-565	>1000	20
Solar Dish- Stirling (SDS)	550-750	>1300	30

A.2. STEG technology

A thermoelectric device consists of both n- and p- type-semiconducting materials connected electrically in series and thermally in parallel.[22-24] Thermoelectric generators (TEG) utilize the Seebeck effect, which generates voltage when one side of the TEG is maintained at a higher temperature compared to the other side, due to the random thermal motion of charge carriers, which cause current to flow when the circuit is closed.[22, 23, 25] As such, thermoelectrics represent reliable solid-state devices that convert heat directly into electricity and vice versa.[26, 27] They are widely used in refrigerators, space applications, remote sensing, electronics cooling, the automobile industry, and have good potential for solar thermal power generation.[28, 29]

The efficiency of a thermoelectric device depends on the materials used. The most important material properties can be lumped into a dimensionless figure of merit (zT) – defined as $zT = (S^2\sigma / \kappa)T$, where S, σ, *k* and T are the Seebeck coefficient, electrical conductivity, thermal conductivity and absolute temperature respectively.[9, 30-32] The numerator, $S^2\sigma$, constitutes to the electrical properties of the materials and is known widely as thermoelectric power factor.[33] The efficiency of an ideal thermoelectric device, η_{TEG}, can be written as a function of the temperatures and the figure of merit, as follows:

$$\eta_{TEG} = \frac{T_H - T_C}{T_H} \frac{\sqrt{1+(zT_M)}-1}{\sqrt{1+(zT_M)}+\frac{T_C}{T_H}} \quad (1)$$

where T_C is the cold-side temperature, T_H is the hot-side temperature, and (zT_M) is the effective figure of merit of the thermoelectric material between T_C and T_H.[9, 32, 34] Considerable global research efforts have been dedicated to enhance the zT of thermoelectric materials.[35-41]

The use of solar thermal technologies for electrical power generation with the help of thermoelectric materials was known since 19th century.[42, 43] Solar Thermoelectric Generators, use a collector, a thermoelectric generator, and a heat sink. Incident solar flux on the thermoelectric generator can be varied with several collector options such as evacuated flat plate; parabolic troughs; Fresnel lenses; and parabolic dishes (as shown in Fig. 1). Heat sink are used a cooling system to dissipate heat from the cold side of the TEG. Recently, instead of using heat sinks, the rejected heat from the cold side of the TEG has been utilized in heating/absorption cooling applications or even for secondary power generation cycles (increasing the overall efficiency of the system),[44, 45] and these modified systems are called as hybrid systems.

STEG *system* efficiency depends on the optical and thermal efficiency of the collector and the zT value of the thermoelectric materials.[46-48] The maximum efficiency for a STEG enclosed in an evacuated glass chamber where hot side coated with a selective absorber coating can be evaluated as follows[46]:

$$\eta_{STEG} = \left[\tau_g \alpha_S \eta_{op} - \frac{\varepsilon_e \sigma_B \left(T_H^{\,4} - T_C^{\,4} \right)}{CR * q_i} \right] * \left[\eta_{TEG} \right] \quad (2)$$

where $\tau_g, \alpha_S, \eta_{op}, \varepsilon_e, \sigma_B$ and q_i are the transmittance of the glass enclosure, absorptance of the selective surface to the solar flux, optical concentration efficiency, effective emittance of the absorber and the envelope, Stephen Boltzmann constant and the incident solar flux, respectively. Effect of enclosing the STEG inside an evacuated chamber is discussed in later in section C1. Improvements in STEG system design can be achieved by increasing the temperature difference across the TEG and/or by reducing the heat loss from the system and by several other means. Materials enhancements can be achieved by increasing the zT values by tuning the materials properties through controlled synthesis techniques.

Fig. 2 shows the STEG efficiency in comparison with the various solar-electricity technologies. It can be seen that the state–of-the-art STEG systems have achieved efficiency only of about 5% for a temperature difference of about 100 °C with the materials zT values of about 1,[9] whereas other solar to electricity conversion (CST & CPV) systems have efficiencies above 18%. Thus the major commercial barrier of STEG technology was its conversion efficiency, which is much lower than other solar-electricity technologies. Despite these traditionally low efficiencies, STEG research is flourishing, and thermoelectric materials are still improving (albeit gradually).[49]

In order for these concepts to move down the technological pipeline from research to commercial deployment, the fundamental aspects of STEG in terms of thermoelectric materials and system design must be well known. In this review, we addressed this challenge by exploring the fundamental progress of STEG technology. As such, this paper presents a critical review of STEG research (particularly recent experimental efforts) and points out strategic research directions, which could allow this technology to evolve. It is found that a staged development where STEGs are added in as topping cycles and/or waste heat scavengers to CST plants presents an excellent opportunity. Depending on future developments in thermoelectric materials, STEGs could eventually be feasible for combined heat and power generation or even stand-alone systems.

B. Development of Thermoelectric materials for Solar Thermal Application

Maria Telkes reported a remarkable STEG system efficiency of 3.35% for the first time in the 1950s.[50] These promising results attracted many researchers to use thermoelectric generator for solar thermal energy conversion.[51, 52] To date, however, the best experimental result for a solar thermoelectric generator had a maximum efficiency of around 5% for a device fabricated by Kraemer et al. using nanostructured thermoelectric materials with zT=1.03.[9] It is obvious from equation 1 that improving the efficiency of solar thermoelectric generators is possible if higher zT materials can be employed.[53]

The parameters that control the zT of thermoelectric materials are Seebeck coefficient S, electrical conductivity σ, and thermal conductivity k (see equation 1). In order to achieve a high figure of merit (zT), the Seebeck coefficient and electrical conductivity should be high and thermal conductivity should be low.[54] Reducing the thermal conductivity, without sacrificing the electrical conductivity or the Seebeck coefficient, however, takes a considerable effort. For metals, or degenerate semiconductors, the Seebeck coefficient is given by equation 3,[54] while the electrical conductivity is given by equation 4.[55]

$$S = \frac{8\pi^2 k_B^2}{3eh^2} m^* T \left(\frac{\pi}{3n}\right)^{\frac{2}{3}} \quad (3)$$

$$\sigma = ne\mu \quad (4)$$

Heat is conducted through the material by two sources, charge carriers (electronic thermal conductivity, k_e) and lattice phonons (Phononic thermal conductivity, k_l) and the thermal conductivity will be low when k_l and k_e are low (see equation 6).[32, 56, 57]

$$k = k_l + k_e \quad (5)$$

$$k_e = Lne\mu T \quad (6)$$

From equations 3-6, we can see that conflicts arise in optimizing the zT of the thermoelectric materials. For an example, if we just concentrate on increasing the Seebeck coefficient, the effective mass (m^*) should be high, but on the other hand the electrical conductivity will be reduced (as mobility, μ is inversely proportional to m*). Recent studies, however, show that the key for achieving higher zT through band structure engineering should be low effective mass along the transport direction.[58] Hence

material scientists are trying to find different ways to optimize the material properties to maximize the zT values.[23, 59, 60]

Different elements from group III-VI and their alloys were studied to have better understanding about the thermoelectric phenomenon, in order to enhance the thermoelectric zT.[61-74] Conventional bulk thermoelectric materials reached their limits of $zT \geq 1$,[75, 76] but recent advances in nanostructured thermoelectric materials have opened the door to obtain higher zT values.[25, 54, 76] The idea of nanostructuring to enhance the thermoelectric effect of materials was first showed by Hicks and Dresselhaus in their theoretical study.[53] Hicks et al. published experimental data verifying this in 1996.[77] They estimated that the zT value can be larger than 2 for PbTe quantum wells confined by a $Pb_{0.927}Eu_{0.073}Te$ barrier layer. Subsequently thermoelectric materials with zT values of ~2 (Bi_2Te_3/Sb_2Te Superlattices Nanodots) and ~2.4 (PbTe/PbTeSe Superlattices) at room temperature have been reported by Harman et al[78] and Venkatasubramanian et al,[79] respectively. A remarkable zT value of ~3 (Bi doped PbSeTe/PbTe Quantum dot Superlattices) at 277 °C was recently reported by Harman et al.[80] However, thermoelectric materials with superlattices and nanodots structures have proven to be challenging for use in large-scale energy-conversion applications, due to restrictions in heat transfer, reproducibility and high manufacturing cost.[81]

Nanocomposites have proven to overcome these problems mentioned above. The most common route of nanocomposite synthesis is a two-step method; high-energy ball milling and hot pressing. Enhancements in zT are attained by effectively reducing the particle size to nano scale dimension.[76, 82] Another technique used to find thermoelectric bulk materials with complex crystal structures to make it efficient, which was first proposed by Slack.[32, 83] Slack suggested that ideal bulk thermoelectric materials should have thermal conductivity like glass and electrical conductivity like a crystal known as phonon-glass electron-crystal (PGEC).[32, 83] Skutterudites and calthrates are the typical materials that exhibit this kind of structure. These materials have intrinsic void in the open cage crystal structure, where by introducing a guest atom or molecule into the void found to reduce the lattice thermal conductivity.[56] Researcher mostly utilized these two techniques over the last two decades to find efficient thermoelectric materials – both of which serve to reduce the lattice thermal conductivity.[54, 82]

Even after several decades of research, the best commercially available bulk thermoelectric materials are bismuth telluride based alloys (maximum zT ~1).[84] Several other materials are proven on a laboratory scale, but are not useful as commercial products. For example, type I calthrates have a peak zT ~1.35 at 627 °C for n-type $Ba_8Ga_{16}Ge_{30}$,[85] but, unfortunately its p-type ($Ba_8Ga_{16}Al_3Ge_{27}$) has a relatively low value zT of ~0.6 at 487 °C.[86] Thus, unless improvements in zT values of p-type calthrates are made, the overall device is unlikely to be significantly better than bismuth telluride. As another example, p-type

β-Zn_4Sb_3 has a tendency to show a decay in its thermoelectric properties upon thermal cycling (a key operational requirement for a solar power system).[87] For many potential thermoelectric materials, rarity in the Earth's crust (e.g. Tellurium) and their demand in other products, raise their prices above levels which would not allow them to be competitive with other technologies like solar photovoltaic cells.[88, 89] Toxicity and other handling issues, also present problems.[33, 88]

In the next section, developments of potential thermoelectric materials like Bi_2Te_3 alloys, PbTe /PbSe alloys, Skutterudites, Half-heuslers compounds and SiGe alloys and its zT enhancements are discussed (shown in Table 2). Followed which, their impact on solar thermoelectric energy conversion is briefed.

Table 2.Materials for Solar Thermoelectric Energy Conversion With $zT \geq 1$

Thermoelectric Material	Type	T°C	zT_{Max}	Year	Ref
BiTe Alloys					
$Bi_2Te_{2.7}Se_{0.3}$	n	125	1.04	2010	90
$Bi_{0.5}Sb_{1.5}Te_3$	p	100	1.40	2008	81
$(BiSb)_2Te_3$	p	167	1.47	2008	91
$Bi_{0.52}Sb_{1.48}Te_3$	p	27	1.56	2009	92
$Bi_{0.48}Sb_{1.52}Te_3$	p	117	1.50	2010	93
$Bi_{0.4}Sb_{1.6}Te_3$	p	43	1.80	2010	94
(0.3 vol.% Al_2O_3)/$Bi_{0.5}Sb_{1.5}Te_3$	p	50	1.50	2013	95
PbTe Alloys					
$AgPb_{18}SbTe_{20}$	n	527	2.20	2004	96
$Pb_{9.6}Sb_{0.2}Te_3Se_7$	n	377	1.20	2006	97
$(Pb_{0.95}Sn_{0.05}Te)_{0.92}(PbS)_{0.08}$	n	369	1.50	2007	98
$K_{0.95}Pb_{20}Sb_{1.2}Te_{22}$	n	477	1.60	2009	99
$Ag_{0.53}Pb_{18}Sb_{1.2}Te_{20}$	n	427	1.70	2009	100
$Ag_{0.5}Pb_6Sn_2Sb_{0.2}Te_{10}$	p	357	1.45	2006	101
$Na_{0.95}Pb_{20}SbTe_{22}$	p	427	1.70	2006	102
$Tl_{0.02}Pb_{0.98}Te$	p	500	1.50	2008	103
2% Na doped PbTe-PbS	p	527	1.80	2011	104
$Pb_{0.98}Na_{0.02}Te_{0.85}Se_{0.15}$	p	577	1.80	2011	105

PbTe–SrTe doped with Na	p	642	2.20	2012	106
PbSe Alloys					
$PbSe:Al_{0.01}$	n	577	1.3	2012	107
Na doped PbSe	p	577	1.2	2011	108
$Pb_{0.92}Sr_{0.08}Se$	-	657	1.5	2014	109
Skutterudites					
$Yb_{0.19}Co_4Sb_{12}$	n	327	1.00	2000	110
$In_{0.25}Co_4Sb_{12}$	n	302	1.20	2006	111
$CoSb_{2.75}Sn_{0.05}Te_{0.20}$	n	550	1.10	2008	112
$Yb_{0.2}Co_4Sb_{12.3}$	n	527	1.30	2008	113
$Na_{0.48}Co_4Sb_{12}$	-	577	1.25	2009	114
$Ba_{0.14}In_{0.23}Co_4Sb_{11.84}$	n	577	1.34	2009	115
$Ba_{0.08}La_{0.05}Yb_{0.04}Co_4Sb_{12}$	n	577	1.70	2011	116
$Sr_{0.12}Ba_{0.18}DD_{0.39}Fe_3CoSb_{12}$	p	527	1.30	2010	117
Half-Heuslers					
$Hf_{0.5}Zr_{0.25}Ti_{0.25}NiSn_{0.99}Sb_{0.01}$	n	500	1	2012	118
$Hf_{0.8}Ti_{0.2}CoSb_{0.8}Sn_{0.2}$	p	800	1	2012	119
Si-Ge Alloys					
$Si_{80}Ge_{20}$	n	900	1.30	2008	120
$Si_{80}Ge_{20}$	p	950	0.95	2008	121

T °C is the temperature where zT max is achieved

B.1. BiTe alloys

The most established material in the field of thermoelectrics is Bi_2Te_3 and its alloys Bi_2Se_3 and Sb_2Te_3.[122] Bismuth and tellurium are heavy elements, which make them suitable for thermoelectrics, since heavy elements have small phonon group velocity, low thermal conductivity, small band gaps and large charge mobility.[55] Experimental results for various bismuth telluride alloys are listed in Table 2. Nanocomposites (p-type $Bi_{0.5}Sb_{1.5}Te_3$ and n-type $Bi_2Te_{2.7}Se_{0.3}$) synthesized by high-energy ball milling and hot pressing achieved a peak value of zT ~1.4 at 100 °C and ~1.04 at 125 °C, respectively. This is

much improved from the baseline bulk material which has a zT~1.[81, 90] Poudel et al. found that the average grain size is 20 nm for p-type $Bi_{0.5}Sb_{1.5}Te_3$.[81] An average grain size of about 1-2 μm was calculated for n-type $Bi_2Te_{2.7}Se_{0.3}$ by Yan et al.[90] The enhanced zT value of p-type $Bi_{0.5}Sb_{1.5}Te_3$ and n-type $Bi_2Te_{2.7}Se_{0.3}$ was achieved, due to the significant reduction in the lattice thermal conductivity by strong boundary scattering (owing to the presence of small grain sizes) of phonon at the interfaces of the nanostructures.[81, 90]

p-type $Bi_{0.48}Sb_{1.52}Te_3$, $Bi_{0.52}Sb_{1.48}Te_3$, 0.3 vol.% Al_2O_3 /$Bi_{0.5}Sb_{1.5}Te_3$ materials, synthesized by spark plasma-sintering method (have zT≥ 1.5 as listed in Table 2), are better than the nanocomposite prepared by high-energy ball milling method.[92, 93, 95] This is because the nanocomposite prepared by spark plasma-sintering method have coherent grain boundaries, whereas nanocomposites prepared by ball milling are random.[92] Inclusion of nanostructured particles in either bulk or nanocomposite materials is known as "nanoinclusion", and has been shown to reduce the lattice thermal conductivity without significantly affecting the thermoelectric power factor.[94] Fan et al., using above technique, synthesized p-type $Bi_{0.4}Sb_{1.6}Te_3$ to make a nanocomposite which consist of 40% nanostructured particles (< 200 nm) and 60% micron -sized particles and reported a high zT value of 1.8 at 43 °C .[94]

Cao et al. utilized a simple hydrothermal technique to synthesize p-type $(BiSb)_2Te_3$, where a zT ~ 1.47 at 165 °C was achieved.[91] Keunákim et al. used a cost effective strain assisted technique to synthesize p-type $Bi_{0.45}Sb_{1.55}Te_3$, where Z was increased by a factor of ~2 over the non-strained samples.[123] Even though the zT values are less for the materials synthesized through these procedures than the highest value of zT attained in Bi_2Te_3, however, these synthesis procedures have a lot of potential due to their simplicity, scalability, and cost effectiveness.

B.2. PbTe and PbSe alloys

PbTe is also a heavy material, like Bi_2Te_3, and its bulk alloy has a zT of ~0.7 at 467 °C. PbTe alloys with PbSe and SnTe exhibited a zT of ~1, were used in power generation.[30, 124] $(AgSbTe_2)_x(PbTe)_{1-x}$ (also known by the acronym LAST) and $(AgSbTe_2)_{1-x}(GeTe)_x$ (known as TAGS) are other classical thermoelectric materials which display very good thermoelectric properties, and have been extensively studied since the 1960s.[30, 54, 125] TAGS, with zT~1.2 p-type, has been employed in power generation for a long time, due to its superior thermal stability over LAST.[54] PbTe and its alloys have been dominant in thermoelectric power generation over the past few decades for temperature above 300 °C.[54, 84]

Experimental results of various PbTe alloys, with respective zT values ranges from 1.20 to 2.20 are listed in Table 2. A peak zT of 2.2 at 527 °C was achieved for n-type $AgPb_{18}SbTe_{20}$ synthesized using the melt growth method.[96] Such high values of zT were achieved through placement of nano precipitates

(Ag and Sb) in the crystal matrix, which enabled a reduction of lattice thermal conductivity.[100, 126] Similar effects were found for n-type $(Pb_{0.95}Sn_{0.05}Te)_{0.92}(PbS)_{0.08}$ and $Ag_{0.53}Pb_{18}Sb_{1.2}Te_{20}$ as well as p-type $Ag_{0.5}Pb_6Sn_2Sb_{0.2}Te_{10}$, $Na_{0.95}Pb_{20}SbTe_{22}$ and 2% Na doped PbTe-PbS.[98, 100-102, 104] Alternatively, enhancement in the thermoelectric power factor found in n-type $Pb_{9.6}Sb_{0.2}Te_3Se_7$ and p-type $Tl_{0.02}Pb_{0.98}Te$ was due multiple valance bands and the introduction of resonant electronic states in the valance band, respectively.[97, 103] Another high value of zT~2.2 at 642 °C was achieved in PbTe–SrTe doped with Na, due to the nanoinclusion of 2–10 nm endotaxial SrTe nanocrystals in Na doped PbTe matrix.[106]

PbSe is considered an alternative to PbTe, since the abundance of Tellurium in the Earth's crust is less than 0.001 ppm, while Selenium is 0.5 ppm.[88] Aluminum doped PbSe (n-type) has a zT of ~1.3 and Sodium doped PbSe (p-type) has a zT of ~1.2 at 577 °C, but both zT values are less than that of good PbTe alloys.[107, 108] Recently, adding small quantities of Sr in PbSe showed that enhances in zT, where maximum zT was ~1.5 at 642°C, was demonstrated by JeffreyáSnyder et al.[109]

B.3. Skutterudites

Skutterudites are another potential thermoelectric material, which has lower thermal conduction due their complex crystal structures and are widely explored for power generation applications.[84] MX_3 is the chemical formula for skutterudites, where M is Co, Rh or Ir and X is P, As or Sb. Because of large voids in the crystal cage structure, it favors incorporation of small guest ions into its intrinsic sites which forms the filled skutterudites ($T_yM_4X_{12}$).[56, 127] T_y, the guest atom in the crystal structure is responsible for strong low frequency phonon scattering, the phenomenon known widely as "rattling effect".[56, 84] Scattering of low frequency phonons through conventional methods is rather difficult.[56] $CoSb_3$ based skutterudites have been studied extensively because of the abundance of the constituent elements and its versatility of accepting various lanthanides, actinides, alkaline earth metals, alkalis, and Group IV elements for use in void-filling.[82, 127] Filled, unfilled and multiple filled Skutterudites that have $zT \geq 1$ is listed in Table 2.[112-117] It has to be noted that nano structuring skutterudites will further decrease the thermal conductivity and a peak value zT ~1.7 at 577 °C reported for n-type $Ba_{0.08}La_{0.05}Yb_{0.04}Co_4Sb_{12}$ synthesized using high-energy ball milling and spark plasma-sintering nano structuring methods.[116] Improvements in the zT values of p-type skutterudites were not in same pace in comparison to its n-type counterpart, because filling tends to push them into strongly towards n-type materials.[128]

B.4. Half-Heuslers

Another promising thermoelectric material which has high thermal stability is half heuslers (HH) compounds.[32] Half heuslers compounds are intermetallic compounds with high Seebeck coefficient and relatively higher thermal conductivity.[32, 84] Higher thermal conductivity in HH is the reason, which

hindered the development of these materials. Conversely, nano structuring of these compounds proved to reduce their lattice thermal conductivity due to phonon scattering. Similar effect is evident in the n-type $Hf_{0.5}Zr_{0.25}Ti_{0.25}NiSn_{0.99}Sb_{0.01}$ synthesized using high-energy ball milling and hot pressing and p-type $Hf_{0.8}Ti_{0.2}CoSb_{0.8}Sn_{0.2}$ synthesized using Arc Melting, high-energy ball milling and hot pressing. These nanostructured materials had a peak zT ~1 at 500 °C and zT ~1 at 800 °C, which was higher than that of their bulk structure.[118, 119]

B.5. SiGe Alloys

SiGe alloys are other important materials, which are suitable for high temperature applications because they have very low degradation, even up to 1000 °C. Bulk $Si_{0.8}Ge_{0.2}$ has a zT of ~1 and 0.6, for n and p-type, respectively.[129] Nanostructured silicon germanium alloys were proven to have an enhanced zT values compared to their bulk alloys. SiGe nanocomposite, prepared by high-energy ball milling and hot Pressing, have zT ~1.3 at 900 °C and zT~1 at 900-950 °C, where its bulk material possess zT ~1 and zT ~0.6.[120, 121] SiGe alloys are costlier than other thermoelectric materials and mostly used in space power applications where solar cells could not be used.[130]

Overall, nanocomposites thermoelectric materials have played a significant role in improving zT values. These materials effectively decrease the thermal conductivity by reducing particle size, which helps to scatter the phonon at the interfaces. In some of the nanocomposite, nanoprecipitate in the crystal matrix tends to scatter low frequency phonons through rattling effect, which reduces the thermal conductivity without significantly affecting the power factor. Thermoelectric power factor on the other hand can be improved by having multiple and/or resonant electronic state in the valance band. Some the bulk thermoelectric materials also found to reduce the thermal conductivity by having complex crystal structure through the rattling effect. Nanocomposite thermoelectric materials could be used in solar thermal power generation applications, if they can be developed cost effective and efficient. These developments would lead to lay the pathway for energy efficient solar conversion technology.

C. Development of solar thermoelectric generator (STEG)

For solar thermal applications, different types of thermoelectric materials with a wide temperature range (from 30 °C to 1000 °C) are available that can be used for power generation. For instance, bismuth telluride alloys can be used in low temperature solar thermal applications (e.g. evacuated tube systems), that can operate from 30 to 200 °C.[9, 131] PbTe/PbSe alloys, skutterudites and half-heuslers compounds can be utilized in the medium temperature solar thermal applications (e.g. parabolic trough and linear Fresnel collectors) that can operate from 200 to 500 °C.[131] For high temperature solar thermal applications (e.g.

solar towers and larger parabolic dishes), SiGe alloys are suitable since they can operate under extreme temperature for long time periods with small degradation in the material properties.[130, 131] This implies that detailed experimental studies on solar thermoelectric generators fabricated using these materials are needed and may lead to develop solar thermoelectric system competitive to solar PV and CST technologies.[4]

Recent developments in the field of thermoelectrics (as discussed above) have attracted many researchers to integrate thermoelectric materials into solar-electricity conversion technologies. These systems can be broadly classified into four types i) non-concentrated STEGs, ii) concentrated STEGs, iii) thermal TEG hybrids, and iv) photovoltaic TEG hybrids. In literature good theoretical design and proposal on STEG are available,[132, 133] however, in the forth-coming sections only prominent experimental works are considered for review. Table 3 shows experimental values of different types of STEG system.

C.1. Non-concentrated and concentrated STEG

The idea of using thermoelectric generator in solar thermal technologies has been an area of interest since 1954, when Telkes published a detailed summary of her remarkable work.[50] Telkes used four different types of thermoelements and found that the most efficient were thermoelements made of a p-type ZnSb (Sn, Ag, Bi) and an n-type 91% Bi+9% Sb. The maximum efficiency of these (zT=0.4) with a double-paned flat plate collector was 0.63% for a 70^{o}C temperature difference across the thermoelements.[50] Using a concentrated system with a lens (50 times optical concentrations), an efficiency of 3.35% was reported for a temperature difference of ~247^{o}C across thermoelements.[50] She also suggested that use of water, as the coolant for the cold side of the thermoelements would provide hot water as the byproduct. Even almost after six decades of research since 1950s, the efficiency of STEG hasn't improved a lot; even some of the STEG systems have efficiency lesser than that of Telkes system. Brief studies on the experimental results of the researchers are presented in this section to show reader about the further scope for improvements in STEG system design.

Table 3. Various experimental results of Solar Thermoelectric generator (flat plate collector–FPC, evacuated flat plate collector–EFPC, conical concentrator–CC, compound parabolic concentrator–CPC, Fresnel lens–FL, dye-sensitized solar cell–DSSC, selective solar absorber-SSA, polymer solar cell–PSC, temperature difference across the thermoelements–ΔT, electrical efficiency– η_{Elec}, thermal efficiency– η_{Th})

System	n-Type	p-Type	ZT_{Max}	ΔT	η_{Elec}	η_{Th}	Year	Ref

Non Concentrating								
FPC	Bi-Sb alloy	ZnSb alloy	0.4	70	0.63	-	1954	50
FPC	Bi-Te alloy	Bi-Te alloy	0.72	70	0.6	-	1980	51
EFPC	Bi-Te alloy	Bi-Te alloy	1.03	100	5.2	-	2011	9
Concentrating								
Lens	Bi-Sb alloy	ZnSb alloy	0.4	247	3.35	-	1954	50
Semi Parabolic	Bi-Te alloy	Bi-Te alloy	0.72	120	0.5	-	1980	51
CC	Bi-Te alloy	Bi-Te alloy	-	100	0.9	-	1998	52
Dish and FL	Bi-Te alloy	Bi-Te alloy	0.41	~150	3	-	2010	134
CPC	$La_{1.98}Sr_{0.02}CuO_4$	$CaMn_{0.98}Nb_{0.02}O_3$	-	600	0.13	-	2011	135
Thermal TEG								
Hybrid								
Parabolic Dish	Bi-Te alloy	Bi-Te alloy	0.6	35	-	11.4	2011	136
EFPC	Bi-Te alloy	Bi-Te alloy	0.59	-	~1	~47	2013	45
Parabolic Mirror	Bi-Te alloy	Bi-Te alloy	0.7	150	5	50	2013	44
Photovoltaic TEG								
Hybrid								
DSSC-SSA-TE	Bi-Te alloy	Bi-Te alloy	-	6	13.8	-	2011	137
Hot Mirror	Bi-Te alloy	Bi-Te alloy	-	20	-	-	2012	138
PSC-TE	Bi-Te alloy	Bi-Te alloy	-	9.5	-	-	2013	139

C.1.1. Experimental Set-ups (collectors)

Experimental results of non-concentrated STEG's, listed in Table 3, show that most of the system used flat plate collector (FPC) as a means to receive the sunlight. Kraemer et al. developed the most efficient collector as shown in Fig. 3, which was able to achieve a temperature difference (ΔT) of about 100 °C across the of thermoelements.[9] Achieving 100 °C was possible in the work of Kraemer et al. because the thermoelements were enclosed inside an evacuated glass chamber (an evacuated flat plate collector (EFPC)), which reduces the heat loss due to convection.[9, 140] Note that Kraemer et al. used a

solar simulator with an AM1.5G filter to achieve 1 kW/m^2 and 1.5 kW/m^2 as the input solar power.[9] Telkes and Goldsmid et al. did not operate their system under vacuum conditions and therefore was only able to achieve a maximum ΔT of about 70 °C.[50, 51]

Different types of concentrating collectors utilized by the researchers are also listed in Table 3. Omer et al. and Suter et al. used a solar simulator, which had a conical concentrator (CC) and compound parabolic concentrator (CPC) with CR of about 6 and 1.4 respectively, to concentrate the radiant light from the simulator source.[52, 135] A 175 W infrared heat lamp was used as the simulator source to achieve a radiant power of about 2W/cm^2 by Omer et al.[52] Suter et al. used a high-pressure argon arc that delivers an external source of intense thermal radiation at the entrance of the CPC to achieve a solar power input of 700 W equivalent to 600 CR.[135] Solar simulators were used in order to have a uniform, repeatable radiation input to the hot side surface of the devices and to allow measurement of the maximum efficiency values in steady state conditions.[52]

Goldsmid et al. used a prototype semi-parabolic concentrator and Amatya et al. used a parabolic dish reflector with a CR of about 4 and 66, respectively. These experimental rigs were able to achieve a temperature difference of about 120 and 150 °C across thermoelements, respectively.[51, 134] Goldsmid et al. used an acrylic cover on the top of the collector to reduce the convection losses.[51]. Amatya et al. used a Fresnel lens (FL) as a secondary concentrator at the focal point of the dish reflector to further intensify the beam which is incident on the surface of the TEG and to reduce the convection losses.[134] The primary reason for employing concentrators, as mentioned above, is to achieve a higher temperature difference across the module. Of course, care should be taken to not exceed the operating temperature of TEG.

C.1.2. Thermoelectric module and solar absorber coating

Thermoelectric materials used in STEG systems play an important role in determining the efficiency of the system, whereas the efficiency of the thermoelectric element depends on the zT and ΔT, which is evident from equation 1. Most of the non-concentrated and concentrated systems listed in Table 3 used TEG made using bulk bismuth telluride alloys having ZT around 0.4 to 0.7, which are most widely available. Goldsmid et al. used a single junction Bi_2Te_3 TEG having nickel-plated ends soldered to copper connectors to withstand a temperature of about 180 °C with an aluminum heat sink.[51] Suter et al. used n-type $La_{1.98}Sr_{0.02}CuO_4$ and p-type $CaMn_{0.98}Nb_{0.02}O_3$ as the thermoelements with Al_2O_3 as the absorber and cooling plates with water cooled system to cool the cavity.[135] Even though Suter et al. used thermoelements with a low ZT, it demonstrates the concept of using a solar cavity-receiver in a 1 kW prototype (consisting of 18 TEG modules).[135] Kraemer et al. used nanostructured thermoelements of n-

and p-type bismuth telluride alloys having a relatively high zT of ~1.03, sandwiched between copper plates.[9]

The hot side of the TEGs in all tests was either painted black or coated with a Selective Solar Absorber (SSA) to improve the absorbance of solar radiation and to reduce the emission losses, which in turn increases the hot side temperature.[52, 134] Goldsmid et al., Omer et al. and Suter et al. used matt black paint, black paint and a graphite coating respectively.[51, 52, 135] Amatya et al. used a SSA consists of silicon polymer as a binder with an oxide pigment with absorptivity and emissivity of about (0.88-0.95) and (0.2-0.4), respectively.[134] Kraemer et al. used a SSA with an absorptivity and emissivity of about 0.94 and 0.5 respectively.[9] Temperature difference across the TEG (SSA coated) is found to be increased by 10% as compared to the ordinary black paints.[134]

C.1.3. Efficiency and cost of the STEG system

Electrical efficiencies (η_{Elec}) of the reviewed non-concentrated and concentrated systems are listed in Table 3. Overall these were in the ranges of 0.13-5.20% with the best non-concentrated collector system.[9] Kraemer et al. achieved a peak efficiency of 4.6% at 1 kW/m^2 and 5.2% at 1.5 kW/m^2 (with the cold side maintained at 20 ^oC.[9] Kraemer et al. estimated the cost of the thermoelectric materials to be about $0.17 per electrical Watt generated and predicted that further reduction is possible by using smaller thermoelements. They also predicted that the efficiency of the system can reach a maximum of 14%, when the materials zT values, optical concentration, and absorber temperature are kept at 2, 10 X and ~300 ^oC, respectively.[9] Though some of the non-concentrated systems utilized thermoelectric material with nominal ZT value, the resulting system efficiencies are lower than those predicted by equation 1.[50, 51] This is due to heat losses in the system that could potentially be improved with good design like Kraemer et al. had used.[9, 50, 51]

Concentrated system developed by Amatya et al. achieved a system efficiency of about 3% with output power of 1.8 W and they have proposed that the use of novel thermoelectric materials such as n-type ErAs:$(InGaAs)_{1-x}(InAlAs)_x$ and p-type $(AgSbTe)_x(PbSnTe)_{1-x}$ with a CR of 120 suns, the conversion efficiency can reach maximum value of 5.6%.[134] Amatya et al. calculated the cost of the module to be about $1.6 per Watt, which is an order of magnitude higher than the thermoelectric material cost estimated by Kraemer et al. The discrepancy is due to the cost of the ceramics used to fabricate the TEG module.[141] However, a very recent and detailed estimate by Yee et al. shows that the cost of the total TEG system could be as low as $0.41 per Watt, which implies that STEG has potential to be competitive with other solar to electricity conversion technologies.[89, 134] Concentrated STEG systems used by Goldsmid et al., Omer et al. and Suter et al. have shown very low system efficiencies than those predicted

by equation 1, because of the use of poor system design as discussed above (in the previous sub sections).[51, 52, 135]

In essence a good STEG should use 1) thermoelectric modules with nominal ZT > 0.7, 2) SSA with absorptivity and emissivity of about (0.88-0.95) and (0.2-0.5), and 3) proper system design to reduce convective losses (e.g. vacuum packaging and/or proper glazing).[9, 134] Also, engineering controls should be in place to ensure the operating temperature of the STEG to not exceed materials limits. Theoretical studies show that the efficiency of thermoelectric materials with zT >2 in the intermediate temperature range (300 to 600 °C) may achieve efficiencies of around 16 to 20%.[106] However, this has yet to be experimentally verified. While competitive stand-alone systems may be forthcoming, hybrid systems where an STEG is added to a conventional power system (as a topping or bottoming generator) are feasible today.

C.2. STEG hybrid system

In order for the STEG to be competent with other solar to electricity conversion technologies, the waste heat from TEG cold side can be utilized for heating water or for running other thermal cycles (power generation or cooling), to compensate for the low electrical efficiency. These systems can be classified as hybrid system.

C.2.1. Thermal TEG hybrid system

Zhang et al. developed a thermal hybrid system (a small pilot project) where a TEG module is placed at one end of an evacuated tube of solar water heater (as shown in Fig. 4).[45] This thermal hybrid system consist of 36 TEG modules integrated with 36 evacuated tubes was successfully commissioned in China for water heating and power generation purpose.[45] The thermal efficiency of this system was about ~47% and electrical efficiency was only about ~1%. Electrical energy output was about 0.19 kWh in addition to the thermal energy, which raised 300-liter tank of water to 55 ^{o}C. The electrical efficiency of this system was reduced mainly due to low ΔT and ZT value of about 0.59 of the TEG module. The total cost of the system was estimated to be about $2,400 with a payback period of around eight years.[45]

Vorobiev et al. developed a thermal hybrid system as shown in Fig. 5.[44] This system used a parabolic mirror, which achieved ΔT of about 150 °C across the TEG. It also used thermosyphon effect (passive heat exchange based on natural convection, which circulates a liquid) for cooling the TEG, which does not require a mechanical pump for circulating the water.[34, 44] Electrical efficiency of this system was about 5% producing the electrical energy output of 0.12 kWh in addition to the thermal

energy output of 1.2 kWh (for raising water temperature to 50 °C in over six hours).[44] A thermal TEG hybrid system developed by Fan et al. used parabolic dish collector, that achieved a thermal efficiency of about 11% and the actual TEG efficiency was not provided. The thermal efficiency of the system was low, which was due to the poor reflector used for fabricating the dish.[136]

The hybrid TEG systems of Vorobiev et al. and Zhang et al. can supply ~1 kW of electrical power.[44, 45] If the collector works at this reported capacity over eight hours of good sunlight (1kW/m^2) per day, it could satisfy 50% of the electricity requirements of a small house, 2kW-h. The thermal energy gathered during these conditions could provide an additional ~14.4 MJ (e.g. a 1m^2 collector area operating at 50% thermal efficiency), which would fulfill the entire domestic hot water need.[44, 45] This implies that with further improvements in materials properties, hybrid TEGs could fully meet the electrical and thermal energy needs for the household. Also it will be one of the STEG designs, which could serve to boost development of efficient STEG technology.

C.2.2. Solar photovoltaic TEG hybrid system

Solar photovoltaic thermoelectric (PV-TEG) hybrid technology was proposed to utilize the entire solar spectrum in order to improve conversion efficiency.[142-147] Only a limited amount of experimental studies on PV-TE have been published (as listed in Table 3). Three different types of PV-TEG are listed in Table 3, all using TEGs made from Bi_2Te_3 alloys. Wang et al. developed a PV-TEG model consists of a series-connected dye-sensitized solar cell (DSSC), a solar selective absorber (SSA) and a thermoelectric generator as shown in the Fig. 6. The whole idea is to utilize both the high and low energy photon for energy conversion with help of DSSC and SSA-TEG configuration.[137] The overall conversion efficiency that was achieved using a PV-TEG system was 13.8%. The power density generated from the PV-TEG system was about 12.8 mW/cm^2, when the temperature difference was around 6 ^oC. However, it was expected that the device performance might increase with further optimization.

Another type of PV-TEG hybrid system developed by Mizoshiri et al. used a hot mirror to separate sunlight into UV to visible solar light for PV and near infrared light for TEG module as shown in Fig. 7.[138] A cylindrical lens was used to concentrate the near infrared light on the thermoelectric module. The thin film TEG used in the system was air-cooled. With temperature difference of about 20 ^oC across the thin film, an open circuit voltage of 78 mV was produced. It was found that hybridization had led to an improvement of about 1.3% compared to the photovoltaic panel alone.[138] Zhang et al. developed the first polymer based PV-TEG for power production as shown in Fig. 8, this system used a P3HT/$IC_{60}B$ for making PV cells [139]. This system was able to produce 9 to 11 mW/cm^2 power density when the temperature difference was about 5 to 9 ^oC.[139]

Most of the PV-TEG hybrid systems are in the initial stages of research. These hybrids are promising, so it is a very challenging area for further research. Higher operating temperature of CPV technologies represents the best platform to integrate a TEG device to achieve outstanding overall conversion efficiency.[148] Also, for CPV-TEG systems, there will still be waste heat from the TEG cold side, which can be used for heating/cooling or secondary power generation. These types of hybrid devices may represent the future of the solar energy conversion, if the cost and system efficiency can be restricted in competitive ranges.

D. Other types of STEGs under development

Some STEGs do not fit into the categories discussed above, but may also provide an interesting opportunity for distributed power generation; these types of system are discussed in this section.

Pavements in summer time reach a maximum of 70 ^{o}C, and represent solar collectors, which have already been installed around the world.[149] The estimated urban (paved) land area is >500,00km^2,[150] and (on average) these surfaces receive ~5 kWh/day, so there is an untapped resource of >3,000 EJ/year. Compared with ~530EJ/year of global primary energy consumption,[151] this represents a sizable energy harvesting opportunity. Hasebe et al. proposed to use heat pipe beneath the road pavements in order to utilize the waste heat from the road pavements. They proposed that water flowing around road pavements could be used as heat transfer fluid to collect heat from the heat pipe, and to provide the thermal energy to the hot side of the TEG, whereas the inlet water was used to cool the cold side.[149] A prototype was built comprising 19 thermoelectric modules (made of bismuth telluride alloy), two heat exchangers and a pump to circulate the water. The pump used in the system utilized the electric power produced by the system, however data provided was not sufficient to justify that it might be efficient or not, when employed in large scale.[149]

Salinity solar ponds are large water bodies, which could absorb and store solar energy and maximum temperature of 80 ^{o}C could be achieved in a cost effective manner.[152, 153] Thermal stratification is achieved in these ponds with three convective regions (upper convective zone (UCZ), lower convective zone (LCZ) and non convective zone (NCZ)) as shown in Fig. 9.[152] Maximum temperature difference of about 40 to 60 ^{o}C could be seen between the UCZ and LCZ. A system was developed by Singh et al. in order to utilize this temperature gradient for power production using TEG and thermosyphon tube in a cost effective manner.[152] Experimental setup of this system is shown in Fig. 10. It can be seen that the thermosyphon tube attached to the thermoelectric generator will provide the necessary heat (which gained from the LCZ) for the hot side and rejected heat from the cold side was taken by the UCZ. The system was able to produce 3.2 watts using 16 TEG with an efficiency of about 1%.[152]

Solar cooking is gaining in popularity (over fossil fuels, and wood/charcoal), since it is environment friendly and cost effective.[154] Kaasjager et al. reported a parabolic trough system (refer the paper for system design) used for solar cooking and electrical power generating in a small amount at the same time. The thermoelectric generator integrated in the system can be used for charging portable electronic devices that require low power. A detailed study of this system recommends further reduction in the heat losses would make this system feasible and efficient for solar cooking and (with power generation as a valuable byproduct).[154]

A unique design, which could generate power in a remote location with thermoelectric generators, was proposed by Attia et al.[155] The concept was to place the TEG between heat exchangers that have different thermal masses, which could respond at a different rate when the environment temperature changes and creates temperature difference required for the TEG. The experimental setup, which has TEG and heat exchangers with different geometries, is shown in Fig. 11. Responses of the system to dynamic environmental changes and varying insulation thickness were studied. From the studies, it was shown that the power produced by the system was in the order of 10^{-4} Watts, indicating the need for a scaled-up version. However, it was recommended that further intense research would lead to make efficient system in a cost effective manner.[155]

In summary, low efficiency of the STEG system is the reason why, these technologies has not been deployed over the years in large power generation application. Recent improvements in the zT values of the thermoelectric nanocomposite materials have shown a huge potential to improve the STEG efficiency (as shown in the Fig. 12). Few cost estimates show that the TEG system cost could be as low as $0.41 per W, which implies that STEG system can be cost competent as well. In hybrid systems, waste heat from the TEG cold side could be potentially used in heating/cooling or secondary power generation, in order to reduce the pay back period for the return in investment. The CPV-TEG and other types of STEG systems are in the initial stages of research, but represent many viable pathways towards the development of a cost effective STEG system.

E. Conclusions and Outlook

Out of various nanostructured materials, nanocomposite thermoelectric materials have shown the most advancement in recent years and have the potential to play an important role in improving the efficiency of the STEG systems. The zT values of the nanocomposite thermoelectric materials available today almost crossed nearly unity for many other thermoelectric materials. However, tailoring the synthesis procedure in such a way that the thermal conductivity can be reduced without significantly affecting the thermopower can further enhance the zT of the thermoelectric materials. It can be seen from

the review that thermoelectric materials in the intermediate temperature ranges would be the suitable and efficient materials for power generation applications. In particular, of PbTe alloys (with overwhelming performance) and skutterudites (with rapidly improving zT values) are the most promising thermoelectric materials for future development in the intermediate temperature ranges from 300 °C to 600 °C (see Fig. 12). Depending on the type of collector used, thermoelectric materials (Bi_2Te_3 alloys, PbTe/PbSe alloys, skutterudites, half-heuslers and SiGe alloys) can be formulated to cover the temperature range between 30 and 1000 °C. We foresee that highly abundant, low costs, thermally stable, and environment friendly thermoelectric materials with high zT values, are needed for future STEG system, in order to compete with other solar energy conversion system.

Various non-concentrated and concentrated STEG systems were critically reviewed, it can be seen that improvement in the material properties, SSA coating and certain heat loss reduction technique have led to achieve a maximum efficiency of about 5%, but still the efficiency values can be further improved by enhancing these parameters. This review also finds that although stand-alone STEG configurations are possible, hybrid configurations are more commercially feasible today. That is, STEG systems are much more likely to be adopted in conjunction with other power cycles and/or in situations where heat outputs can be utilized. We propose that the efficient thermoelectric materials with high zT values must be utilized, especially for the medium temperature STEGs (200-600 °C), in order to exploit the inherent advantages of the STEGs to compete with other cost effective solar to electricity conversion systems. We expect that the thermal TEG hybrid and the CPV-TEG (largely unexplored) systems might enable a step-change in the technology in the near future, if global efforts are taken to further intensify the research on these systems.

References:

1. A. Mojiri, R. Taylor, E. Thomsen and G. Rosengarten, *Renew Sust Energ Rev*, 2013, **28**, 654-663.
2. S. Mekhilef, R. Saidur and A. Safari, *Renew Sust Energ Rev*, 2011, **15**, 1777-1790.
3. N. S. Lewis and G. Crabtree, *Basic Research Needs for Solar Energy Utilization- Report of the Basic Energy Sciences Workshop on Solar Energy Utilization. DOE Office of Science*, April 18-21, 2005; available at http://www.er.doe.gov/bes/reports/abstracts.html.
4. M. Xie and D. M. Gruen, *J Phys Chem B*, 2010, **114**, 14339-14342.
5. M. Ortega, P. del Río and E. A. Montero, *Renew Sust Energ Rev*, 2013, **27**, 294-304.
6. A. Ummadisingu and M. S. Soni, *Renew Sust Energ Rev*, 2011, **15**, 5169-5175.
7. S. A. Kalogirou, *Progr Energy Combust Sci*, 2004, **30**, 231-295.
8. G. W. Crabtree and N. S. Lewis, *Phys Today*, 2007, **60**, 37-42.
9. D. Kraemer, B. Poudel, H.-P. Feng, J. C. Caylor, B. Yu, X. Yan, Y. Ma, X. Wang, D. Wang and A. Muto, *Nat Mater*, 2011, **10**, 532-538.
10. R. A. Taylor and G. L. Solbrekken, *IEEE Transaction on Components and Packaging Technologies*, 2008, **31**, 23-31.
11. B. Parida, S. Iniyan and R. Goic, *Renew Sust Energ Rev*, 2011, **15**, 1625-1636.
12. H. L. Zhang, J. Baeyens, J. Degrève and G. Cacères, *Renew Sust Energ Rev*, 2013, **22**, 466-481.
13. M. A. Green, K. Emery, Y. Hishikawa, W. Warta and E. D. Dunlop, *Progr Photovoltaics: Res Appl*, 2014, **22**, 1-9.
14. *Renewable Energy Technologies - Cost analysis series (PV). Int Energy Agency*, 2012; available at http://www.irena.org.
15. S. Kuravi, J. Trahan, D. Y. Goswami, M. M. Rahman and E. K. Stefanakos, *Progr Energy Combust Sci*, 2013, **39**, 285-319.
16. D. Y. Goswami, F. Kreith and J. F. Kreider, *Principles of solar engineering*, CRC PressI Llc, 2000.
17. J. Mariyappan and D. Anderson, *Solar Thermal thematic review. SolarPACES Annual Report*, 2001.
18. W. T. Xie, Y. J. Dai, R. Z. Wang and K. Sumathy, *Renew Sust Energ Rev*, 2011, **15**, 2588-2606.
19. A. Fernández-García, E. Zarza, L. Valenzuela and M. Pérez, *Renew Sust Energ Rev*, 2010, **14**, 1695-1721.
20. M. H. Ahmadi, A. H. Mohammadi, S. Dehghani and M. A. Barranco-Jiménez, *Energy Convers Manage*, 2013, **75**, 438-445.
21. S. H. Alawaji, *Renew Sust Energ Rev*, 2001, **5**, 59-77.
22. F. J. DiSalvo, *Sci*, 1999, **285**, 703-706.
23. J.-c. Zheng, *Front Phys China*, 2008, **3**, 269-279.
24. H. Xi, L. Luo and G. Fraisse, *Renew Sust Energ Rev*, 2007, **11**, 923-936.
25. P. Vaqueiro and A. V. Powell, *J Mater Chem*, 2010, **20**, 9577-9584.
26. J. R. Lim, J. F. Whitacre, J. P. Fleurial, C. K. Huang, M. A. Ryan and N. V. Myung, *Adv Mater*, 2005, **17**, 1488-1492.
27. F. Meng, L. Chen and F. Sun, *Int J Energy Env*, 2012, **3**, 137-150.
28. H. Scherrer, L. Vikhor, B. Lenoir, A. Dauscher and P. Poinas, *J Power Sources*, 2003, **115**, 141-148.
29. N. Vatcharasathien, J. Hirunlabh, J. Khedari and M. Daguenet, *Int J Sust Energy*, 2005, **24**, 115-127.
30. T. M. Tritt and M. Subramanian, *MRS Bull*, 2006, **31**, 188-198.
31. G. Min, *J Electron Mater*, 2010, **39**, 1782-1785.
32. W. Xie, A. Weidenkaff, X. Tang, Q. Zhang, J. Poon and T. M. Tritt, *Nanomaterials*, 2012, **2**, 379-412.

33. M. Hamid Elsheikh, D. A. Shnawah, M. F. M. Sabri, S. B. M. Said, M. Haji Hassan, M. B. Ali Bashir and M. Mohamad, *Renew Sust Energ Rev*, 2014, **30**, 337-355.
34. E. Chávez-Urbiola, Y. V. Vorobiev and L. Bulat, *Sol Energy*, 2012, **86**, 369-378.
35. A. Soni, Z. Yanyuan, Y. Ligen, M. K. K. Aik, M. S. Dresselhaus and Q. Xiong, *Nano Lett*, 2012, **12**, 1203-1209.
36. Y. Zhang, M. L. Snedaker, C. S. Birkel, S. Mubeen, X. Ji, Y. Shi, D. Liu, X. Liu, M. Moskovits and G. D. Stucky, *Nano Lett*, 2012, **12**, 1075-1080.
37. S. Wang, X. Tan, G. Tan, X. She, W. Liu, H. Li, H. Liu and X. Tang, *J Mater Chem*, 2012, **22**, 13977-13985.
38. T. Zhang, J. Jiang, Y. Xiao, Y. Zhai, S. Yang and G. Xu, *J Mater Chem A*, 2013, **1**, 966-969.
39. L. Ivanova, L. Petrova, Y. V. Granatkina, V. Leontyev, A. Ivanov, S. Varlamov, Y. P. Prilepo, A. Sychev, A. Chuiko and I. Bashkov, *Inorg Mater*, 2013, **49**, 120-126.
40. H. Sevinçli, C. Sevik, T. Çağın and G. Cuniberti, *Sci Rep*, 2013, **3**, http://dx.doi.org/10.1038/srep01355.
41. M. Ioannou, G. Polymeris, E. Hatzikraniotis, A. Khan, K. Paraskevopoulos and T. Kyratsi, *J Electron Mater*, 2013, **42**, pp 1827-1834.
42. E. Weston, United States Patent US389124 A, 1888 Sep 4.
43. L. Weinstein, K. McEnaney and G. Chen, *J Appl Phys*, 2013, **113**, 164504.
44. Y. Vorobiev, *Int J Photoenergy*, 2013, **2013**, http://dx.doi.org/10.1155/2013/704087.
45. M. Zhang, L. Miao, Y. P. Kang, S. Tanemura, C. A. Fisher, G. Xu, C. X. Li and G. Z. Fan, *Appl Energy*, 2013, **109**, 51-59.
46. G. Chen, *J Appl Phys*, 2011, **109**, 104908.
47. W. He, Y. Su, S. B. Riffat, J. Hou and J. Ji, *Appl Energy*, 2011, **88**, 5083-5089.
48. L. L. Baranowski, G. J. Snyder and E. S. Toberer, *Energy Environ Sci*, 2012, **5**, 9055-9067.
49. J. Karni, *Nature materials*, 2011, **10**, 481-482.
50. M. Telkes, *J Appl Phys*, 1954, **25**, 765.
51. H. Goldsmid, J. Giutronich and M. Kaila, *Sol Energy*, 1980, **24**, 435-440.
52. S. Omer and D. Infield, *Sol Energy Mater Sol Cells*, 1998, **53**, 67-82.
53. L. Hicks and M. Dresselhaus, *Phys Rev B*, 1993, **47**, 12727.
54. G. J. Snyder and E. S. Toberer, *Nature materials*, 2008, **7**, 105-114.
55. A. Bulusu and D. Walker, *Superlattices Microstruct*, 2008, **44**, 1-36.
56. T. M. Tritt, *Thermal conductivity:– theory, properties and applications*, Kluwer Academic/Plenum Publishers, Dordrecht, 2004.
57. N. Yang, X. Xu, G. Zhang and B. Li, *AIP Adv*, 2012, **2**, 041410.
58. Y. Pei, A. D. LaLonde, H. Wang and G. J. Snyder, *Energy Environ Sci*, 2012, **5**, 7963-7969.
59. G. J. Snyder, M. Christensen, E. Nishibori, T. Caillat and B. B. Iversen, *Nature materials*, 2004, **3**, 458-463.
60. C. B. Vining, *Nature materials*, 2009, **8**, 83-85.
61. N. Mott, *Proceedings of the Royal Society of London. Series A-Mathematical and Physical Sciences*, 1936, **156**, 368-382.
62. R. L. Powell, W. J. Hall and H. M. Roder, *J Appl Phys*, 1960, **31**, 496-503.
63. C. Bradley, *Philoso Mag*, 1962, **7**, 1337-1347.
64. D. MacDonald, W. Pearson and I. Templeton, *Proceedings of the Royal Society of London. Series A. Mathematical and Physical Sciences*, 1962, **266**, 161-184.
65. J. Perron, *Adv Phys*, 1967, **16**, 657-666.
66. M. Vedernikov, *Adv Phys*, 1969, **18**, 337-370.
67. A. K. Sinha, *Phys Rev B*, 1970, **1**, 4541.
68. R. Huebener, *Solid State Phys*, 1972, **27**, 63-134.
69. P. Nielsen and P. Taylor, *Phys Rev B*, 1974, **10**, 4061.

70. M. Baibich, W. Muir, G. Belanger, J. Destry, H. Elzinga and P. Schroeder, *Phys Rev A*, 1979, **73**, 328-330.
71. B. Gallagher, *J Phys F: Met Phys*, 1981, **11**, L207.
72. B. Gallagher and D. Greig, *J Phys F: Met Phys*, 1982, **12**, 1721.
73. C. Domenicali and F. Otter, *Phys Rev*, 1954, **95**, 1134.
74. J. S. Dugdale, *The electrical properties of disordered metals*, Cambridge University Press Cambridge, 1995.
75. M. S. Dresselhaus, G. Chen, M. Y. Tang, R. Yang, H. Lee, D. Wang, Z. Ren, J. P. Fleurial and P. Gogna, *Adv Mater*, 2007, **19**, 1043-1053.
76. A. Minnich, M. Dresselhaus, Z. Ren and G. Chen, *Energy Environ Sci*, 2009, **2**, 466-479.
77. L. Hicks, T. Harman, X. Sun and M. Dresselhaus, *Phys Rev B*, 1996, **53**, R10493-R10496.
78. T. Harman, P. Taylor, M. Walsh and B. LaForge, *Sci*, 2002, **297**, 2229-2232.
79. R. Venkatasubramanian, E. Siivola, T. Colpitts and B. O'quinn, *Nat*, 2001, **413**, 597-602.
80. T. Harman, M. Walsh and G. Turner, *J Electron Mater*, 2005, **34**, L19-L22.
81. B. Poudel, Q. Hao, Y. Ma, Y. Lan, A. Minnich, B. Yu, X. Yan, D. Wang, A. Muto and D. Vashaee, *Sci*, 2008, **320**, 634-638.
82. Z. G. Chen, G. Han, L. Yang, L. Cheng and J. Zou, *Progr Nat Sci Mater Int*, 2012, **22**, 535–549.
83. X. Shi, L. Xi, J. Fan, W. Zhang and L. Chen, *Chem Mater*, 2010, **22**, 6029-6031.
84. W. Liu, X. Yan, G. Chen and Z. Ren, *Nano Energy*, 2012, **1**, 42-56.
85. A. Saramat, G. Svensson, A. Palmqvist, C. Stiewe, E. Mueller, D. Platzek, S. Williams, D. Rowe, J. Bryan and G. Stucky, *J Appl Phys*, 2006, **99**, 023708.
86. S. Deng, X. Tang, P. Li and Q. Zhang, *J Appl Phys*, 2008, **103**, 073503.
87. B. B. Iversen, *J Mater Chem*, 2010, **20**, 10778-10787.
88. R. Amatya and R. J. Ram, *J Electron Mater*, 2012, **41**, 1011-1019.
89. S. K. Yee, S. LeBlanc, K. E. Goodson and C. Dames, *Energy Environ Sci*, 2013, **6**, 2561-2571.
90. X. Yan, B. Poudel, Y. Ma, W. Liu, G. Joshi, H. Wang, Y. Lan, D. Wang, G. Chen and Z. Ren, *Nano Lett*, 2010, **10**, 3373-3378.
91. Y. Cao, X. Zhao, T. Zhu, X. Zhang and J. Tu, *Appl Phys Lett*, 2008, **92**, 143106.
92. W. Xie, X. Tang, Y. Yan, Q. Zhang and T. M. Tritt, *Appl Phys Lett*, 2009, **94**, 102111.
93. W. Xie, J. He, H. J. Kang, X. Tang, S. Zhu, M. Laver, S. Wang, J. R. Copley, C. M. Brown and Q. Zhang, *Nano Lett*, 2010, **10**, 3283-3289.
94. S. Fan, J. Zhao, J. Guo, Q. Yan, J. Ma and H. H. Hng, *Appl Phys Lett*, 2010, **96**, 182104.
95. K. T. Kim and G. H. Ha, *J NanoMater*, 2013, **2013**.
96. K. F. Hsu, S. Loo, F. Guo, W. Chen, J. S. Dyck, C. Uher, T. Hogan, E. Polychroniadis and M. G. Kanatzidis, *Sci*, 2004, **303**, 818-821.
97. P. F. Poudeu, J. D'Angelo, H. Kong, A. Downey, J. L. Short, R. Pcionek, T. P. Hogan, C. Uher and M. G. Kanatzidis, *J Am Chem Soc*, 2006, **128**, 14347-14355.
98. J. Androulakis, C.-H. Lin, H.-J. Kong, C. Uher, C.-I. Wu, T. Hogan, B. A. Cook, T. Caillat, K. M. Paraskevopoulos and M. G. Kanatzidis, *J Am Chem Soc*, 2007, **129**, 9780-9788.
99. P. F. P. Poudeu, A. Guéguen, C.-I. Wu, T. Hogan and M. G. Kanatzidis, *Chem Mater*, 2009, **22**, 1046-1053.
100. B. A. Cook, M. J. Kramer, J. L. Harringa, M. K. Han, D. Y. Chung and M. G. Kanatzidis, *Adv Funct Mater*, 2009, **19**, 1254-1259.
101. J. Androulakis, K. F. Hsu, R. Pcionek, H. Kong, C. Uher, J. J. D'Angelo, A. Downey, T. Hogan and M. G. Kanatzidis, *Adv Mater*, 2006, **18**, 1170-1173.
102. P. F. Poudeu, J. D'Angelo, A. D. Downey, J. L. Short, T. P. Hogan and M. G. Kanatzidis, *Angew Chem*, 2006, **118**, 3919-3923.
103. J. P. Heremans, V. Jovovic, E. S. Toberer, A. Saramat, K. Kurosaki, A. Charoenphakdee, S. Yamanaka and G. J. Snyder, *Sci*, 2008, **321**, 554-557.

104. S. N. Girard, J. He, X. Zhou, D. Shoemaker, C. M. Jaworski, C. Uher, V. P. Dravid, J. P. Heremans and M. G. Kanatzidis, *J Am Chem Soc*, 2011, **133**, 16588-16597.
105. Y. Pei, X. Shi, A. LaLonde, H. Wang, L. Chen and G. J. Snyder, *Nat*, 2011, **473**, 66-69.
106. K. Biswas, J. He, I. D. Blum, C.-I. Wu, T. P. Hogan, D. N. Seidman, V. P. Dravid and M. G. Kanatzidis, *Nat*, 2012, **489**, 414-418.
107. Q. Zhang, H. Wang, W. Liu, H. Wang, B. Yu, Q. Zhang, Z. Tian, G. Ni, S. Lee and K. Esfarjani, *Energy Environ Sci*, 2012, **5**, 5246-5251.
108. H. Wang, Y. Pei, A. D. LaLonde and G. J. Snyder, *Adv Mater*, 2011, **23**, 1366-1370.
109. H. Wang, Z. M. Gibbs, Y. Takagiwa and G. J. Snyder, *Energy Environ Sci*, 2014, **7**, 804-811.
110. G. Nolas, M. Kaeser, R. Littleton and T. Tritt, *Appl Phys Lett*, 2000, **77**, 1855-1857.
111. T. He, J. Chen, H. D. Rosenfeld and M. Subramanian, *Chem Mater*, 2006, **18**, 759-762.
112. W. S. Liu, B. P. Zhang, L. D. Zhao and J. F. Li, *Chem Mater*, 2008, **20**, 7526-7531.
113. H. Li, X. Tang, Q. Zhang and C. Uher, *Appl Phys Lett*, 2008, **93**, 252109.
114. Y. Pei, J. Yang, L. Chen, W. Zhang, J. Salvador and J. Yang, *Appl Phys Lett*, 2009, **95**, 042101.
115. W. Zhao, P. Wei, Q. Zhang, C. Dong, L. Liu and X. Tang, *J Am Chem Soc*, 2009, **131**, 3713-3720.
116. X. Shi, J. Yang, J. R. Salvador, M. Chi, J. Y. Cho, H. Wang, S. Bai, J. Yang, W. Zhang and L. Chen, *J Am Chem Soc*, 2011, **133**, 7837-7846.
117. G. Rogl, A. Grytsiv, P. Rogl, E. Bauer, M. Kerber, M. Zehetbauer and S. Puchegger, *Intermetallics*, 2010, **18**, 2435-2444.
118. G. Joshi, T. Dahal, S. Chen, H. Wang, J. Shiomi, G. Chen and Z. Ren, *Nano Energy*, 2012.
119. X. Yan, W. Liu, H. Wang, S. Chen, J. Shiomi, K. Esfarjani, H. Wang, D. Wang, G. Chen and Z. Ren, *Energy Environ Sci*, 2012, **5**, 7543-7548.
120. X. W. Wang, H. Lee, Y. C. Lan, G. H. Zhu, G. Joshi, D. Z. Wang, J. Yang, A. J. Muto, M. Y. Tang, J. Klatsky, S. Song, M. S. Dresselhaus, G. Chen and Z. F. Ren, *Appl Phys Lett*, 2008, **93**, 193121.
121. G. Joshi, H. Lee, Y. Lan, X. Wang, G. Zhu, D. Wang, R. W. Gould, D. C. Cuff, M. Y. Tang and M. S. Dresselhaus, *Nano Lett*, 2008, **8**, 4670-4674.
122. H. Goldsmid and R. Douglas, *Br J Appli Phys*, 1954, **5**, 386.
123. S. KeunáKim, *Phys Chem Chem Phys*, 2014, **16**, 3529-3533.
124. Z. Dughaish, *Physica B: Condens Matte*, 2002, **322**, 205-223.
125. J. R. Salvador, J. Yang, X. Shi, H. Wang and A. Wereszczak, *J Solid State Chem*, 2009, **182**, 2088-2095.
126. D. Medlin and G. Snyder, *Curr Opin Colloid Interface Sci*, 2009, **14**, 226-235.
127. S. Bai, X. Shi and L. Chen, *Appl Phys Lett*, 2010, **96**, 202102.
128. Z. Tian, S. Lee and G. Chen, *J Heat Transf*, 2013, **135**, 061605.
129. C. B. Vining, W. Laskow, J. O. Hanson, R. R. Van der Beck and P. D. Gorsuch, *J Appl Phys*, 1991, **69**, 4333-4340.
130. M. S. El-Genk, H. H. Saber and T. Caillat, *Energy Convers Manage*, 2003, **44**, 1755-1772.
131. D. Mills, *Sol Energy*, 2004, **76**, 19-31.
132. P. Li, L. Cai, P. Zhai, X. Tang, Q. Zhang and M. Niino, *J Electron Mater*, 2010, **39**, 1522-1530.
133. T. Yang, J. Xiao, P. Li, P. Zhai and Q. Zhang, *J Electron Mater*, 2011, **40**, 967-973.
134. R. Amatya and R. Ram, *J Electron Mater*, 2010, **39**, 1735-1740.
135. C. Suter, P. Tomeš, A. Weidenkaff and A. Steinfeld, *Sol Energy*, 2011, **85**, 1511-1518.
136. H. Fan, R. Singh and A. Akbarzadeh, *J Electron Mater*, 2011, **40**, 1311-1320.
137. N. Wang, L. Han, H. He, N.-H. Park and K. Koumoto, *Energy Environ Sci*, 2011, **4**, 3676.
138. M. Mizoshiri, M. Mikami and K. Ozaki, *Jpn J Appl Phys*, 2012, **51**.
139. Y. Zhang, J. Fang, C. He, H. Yan, Z. Wei and Y. Li, *J Phys Chem C*, 2013, **117**, 24685-24691.
140. M. Zebarjadi, K. Esfarjani, M. Dresselhaus, Z. Ren and G. Chen, *Energy Environ Sci*, 2012, **5**, 5147-5162.

141. S. LeBlanc, S. K. Yee, M. L. Scullin, C. Dames and K. E. Goodson, *Renew Sust Energ Rev*, 2014, **32**, 313-327.
142. Y. Vorobiev, J. Gonzalez-Hernandez, P. Vorobiev and L. Bulat, *Sol Energy*, 2006, **80**, 170-176.
143. D. Kraemer, L. Hu, A. Muto, X. Chen, G. Chen and M. Chiesa, *Appl Phys Lett*, 2008, **92**, 243503.
144. Y. Li, S. Witharana, H. Cao, M. Lasfargues, Y. Huang and Y. Ding, *Particuology*, 2013, http://dx.doi.org/10.1016/j.partic.2013.08.003.
145. T. Liao, B. Lin and Z. Yang, *Int J Therm Sci*, 2014, **77**, 158-164.
146. M. Fisac, F. X. Villasevil and A. M. López, *J Power Sources*, 2014, **252**, 264-269.
147. X. Zhang, X. Zhao, S. Smith, J. Xu and X. Yu, *Renew Sust Energ Rev*, 2012, **16**, 599-617.
148. C. Y. Lu, European Patent EP2660880 A2, 2012 Apr 15.
149. M. Hasebe, Y. Kamikawa and S. Meiarashi, in *International Conference on Thermoelectrics*, IEEE, Vienna, 2006, pp. 697-700.
150. A. Schneider, M. A. Friedl and D. Potere, *Env Res Lett*, 2009, **4**, 044003.
151. *Key World Energy Statistics. Int Energy Agency*, 2012; available at http://www.irena.org.
152. R. Singh, S. Tundee and A. Akbarzadeh, *Sol Energy*, 2011, **85**, 371-378.
153. K. R. Ranjan and S. C. Kaushik, *Renew Sust Energ Rev*, 2014, **32**, 123-139.
154. A. Kaasjager and G. Moeys, in *Global Humanitarian Technology Conference*, IEEE, Seattle, WA, 21-24, October 2012, pp. 6-11.
155. P. M. Attia, M. R. Lewis, C. C. Bomberger, A. K. Prasad and J. M. Zide, *Energy*, 2013, **60**, 453-456.

Figure Captions:

Fig. 1. Solar thermoelectric generator deployed in different solar thermal systems

Fig. 2. Comparison of STEG Efficiency with various other solar-electricity technologies (STEG – Solar Thermoelectric Generator, LFL – Linear Fresnel lens, PTC – Parabolic Trough Collector, ST – Solar Tower, SDS – Solar Dish Stirling, CPV – Concentrated Photovoltaic): ref. 9, 13, 15

Fig. 3. Solar thermoelements enclosed in an evacuated tube. Reproduced with permission from The Royal society of chemistry: ref. 140 ©2012 The Royal society of chemistry

Fig. 4. The structure of an evacuated glass tube with TEG integrated. (a) A glass tube with TEG integrated between the condensation segment and the water jacket segment (temperature difference between this two segment is used for power generation by the TEG), (b) schematic cross-section of the evacuated tube, and (c) top section of the tube with external tube, inner tube and fins removed to reveal the heat pipe. Reproduced with permission from Elsevier: ref. 45 ©2013 Elsevier

Fig. 5. Photograph of Parabolic Mirror with combined cogeneration of heat and electricity. Reproduced from with permission from Hindawi: ref. 44 ©2013 Hindawi

Fig. 6. Schematics of novel PV–TE hybrid device. Reproduced with permission from The Royal society of chemistry: ref. 137 ©2011 The Royal society of chemistry

Fig. 7. Schematics of thermal–photovoltaic hybrid generator. Reproduced with permission form The Japan Society of Applied Physics: ref. 138 ©2012 The Japan Society of Applied Physics

Fig. 8. Polymer Solar Cells – Thermoelectric Generator model. Reproduced with permission form American Chemical Society: ref. 139 ©2013 American Chemical Society

Fig. 9. Schematics of salinity solar pond. Reproduced with permission from Elsevier: ref. 152 © 2011 Elsevier

Fig. 10. Schematics of the experimental setup of solar pond with thermosyphon tube and TEG. Reproduced with permission from Elsevier: ref. 152 © 2011 Elsevier

Fig. 11. Experimental setup of thermoelectric generator with different geometries. Reproduced with permission from Elsevier: ref. 155 © 2013 Elsevier

Fig. 12. Development of zT (materials and STEG) and STEG efficiency (non-concentrated STEG system) over the years: ref. 9, 50, 52, 91, 98, 100-104, 106, 111, 113, 115-117

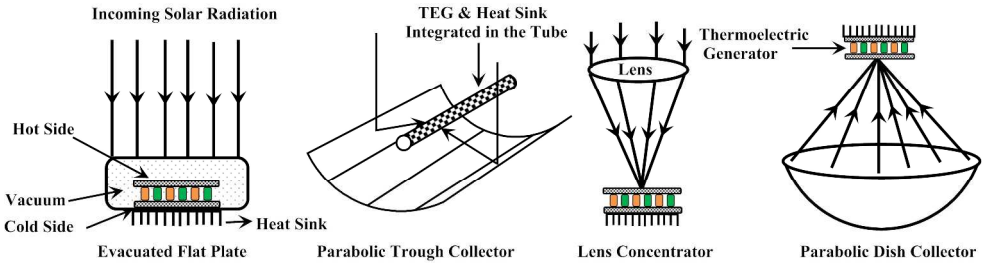

1436x391mm (72 x 72 DPI)

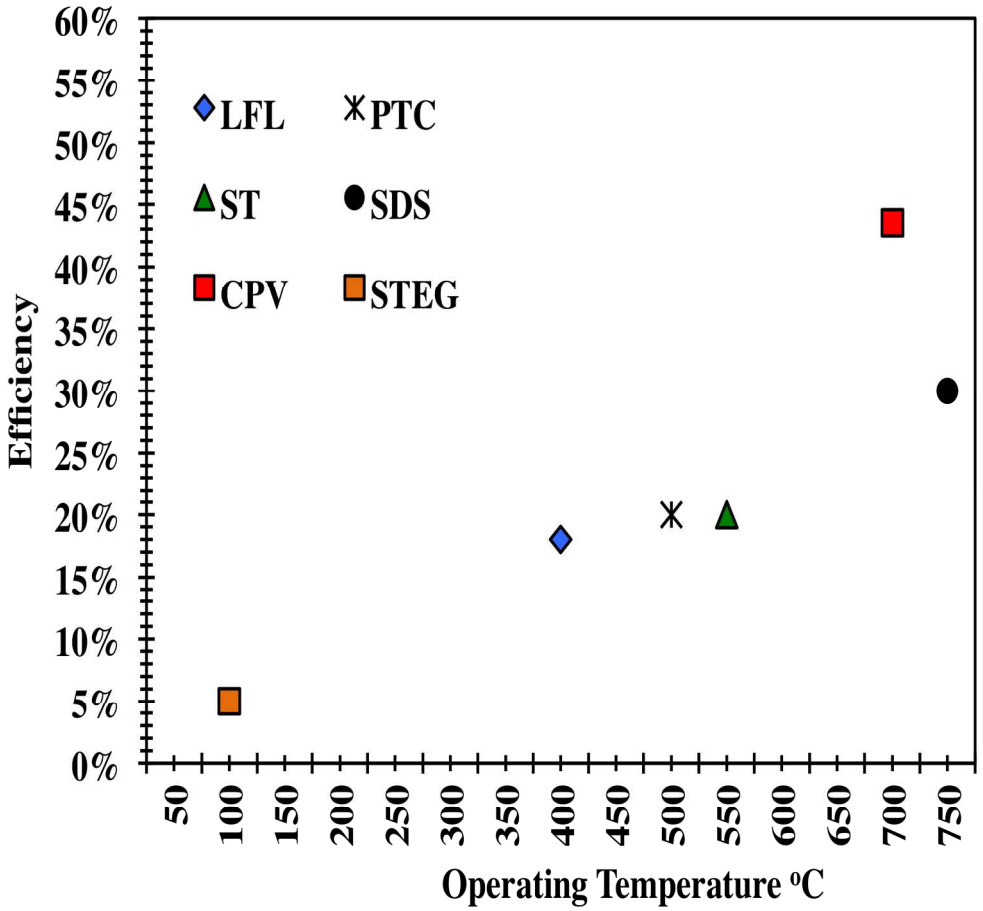

733x684mm (72 x 72 DPI)

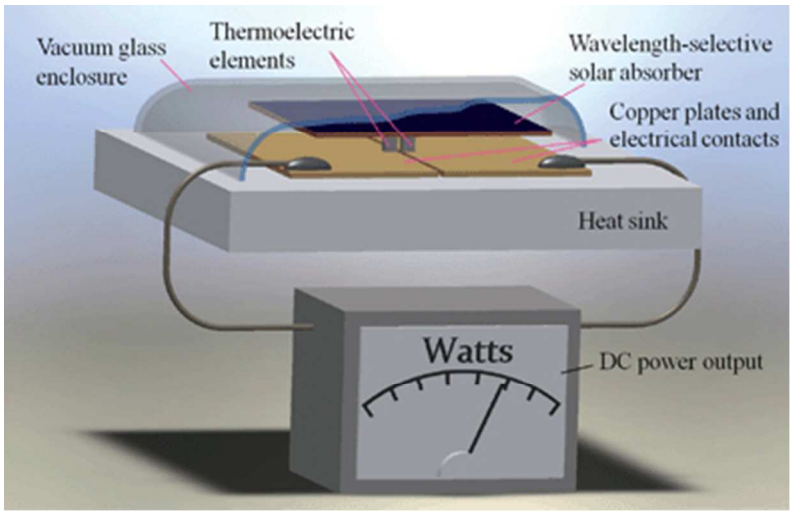

138x88mm (72 x 72 DPI)

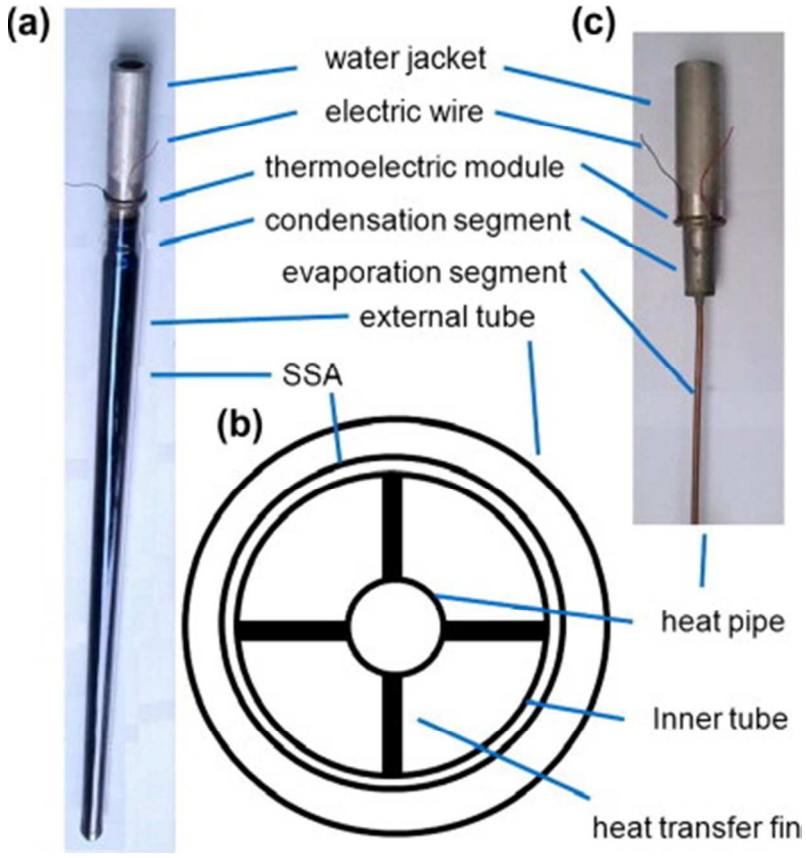

89x95mm (113 x 113 DPI)

50x51mm (300 x 300 DPI)

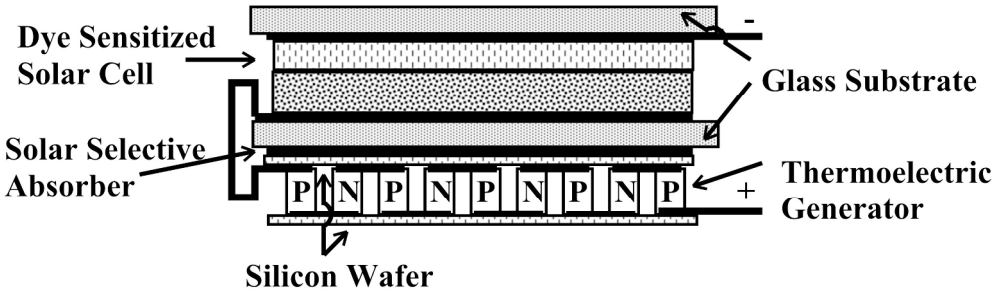

970x299mm (72 x 72 DPI)

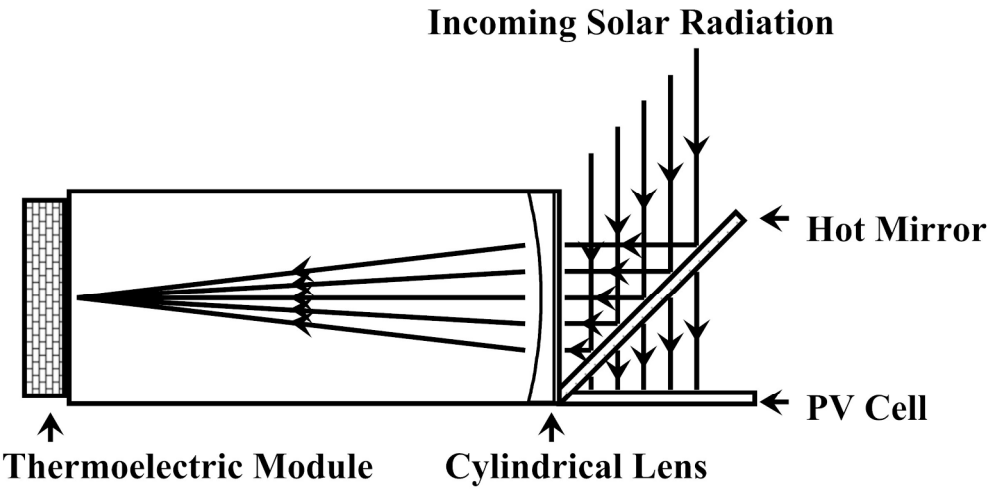

848x426mm (72 x 72 DPI)

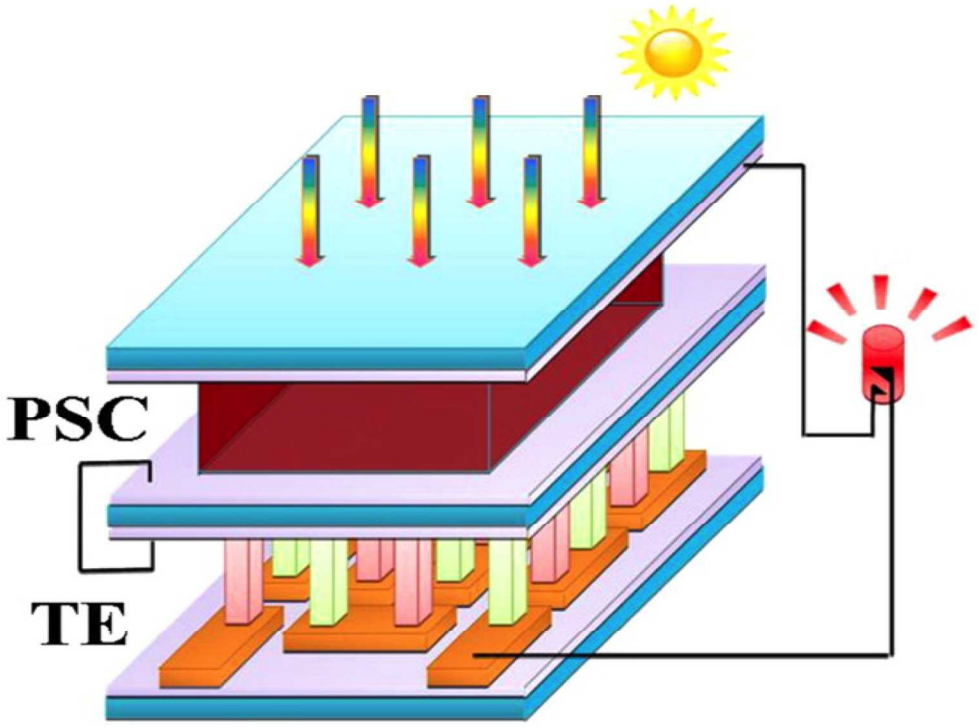

733x550mm (72 x 72 DPI)

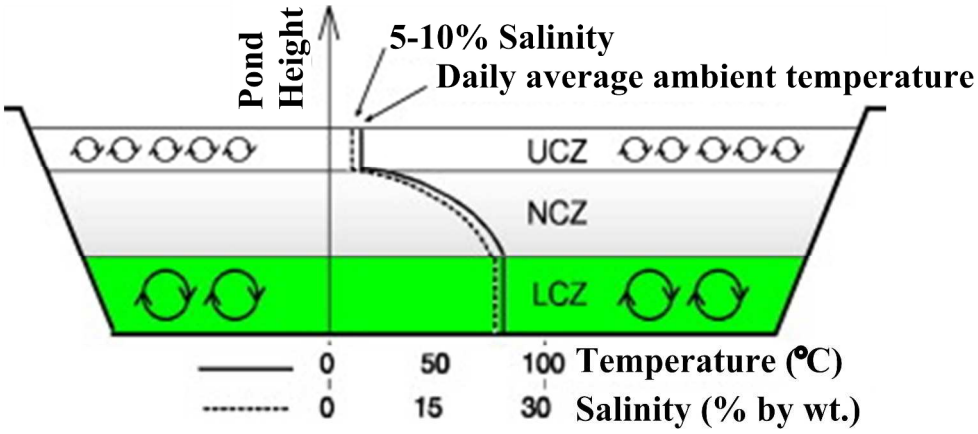

1428x639mm (72 x 72 DPI)

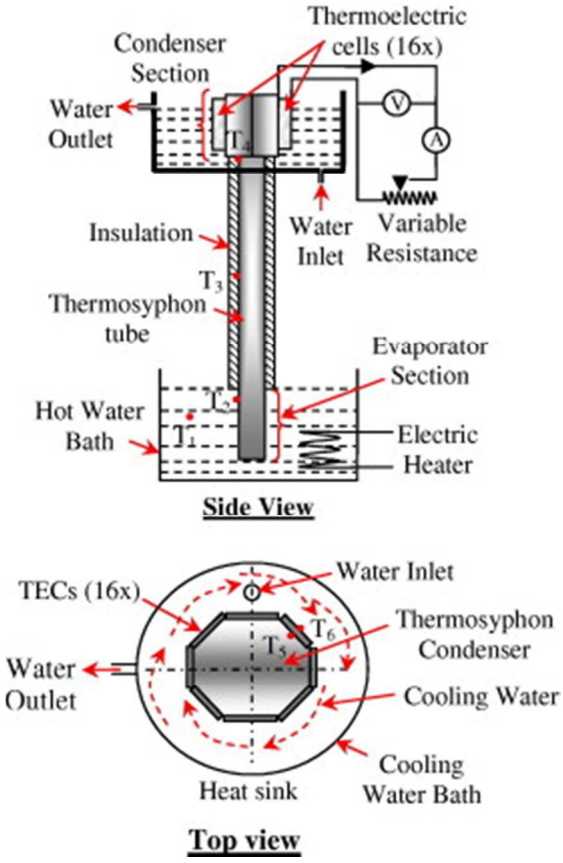

62x95mm (113 x 113 DPI)

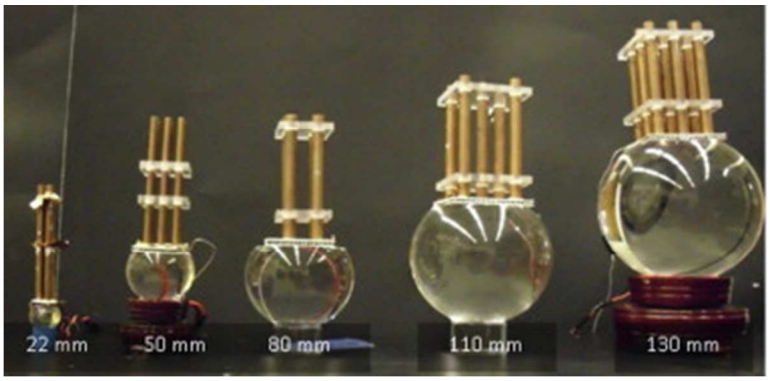

85x41mm (113 x 113 DPI)

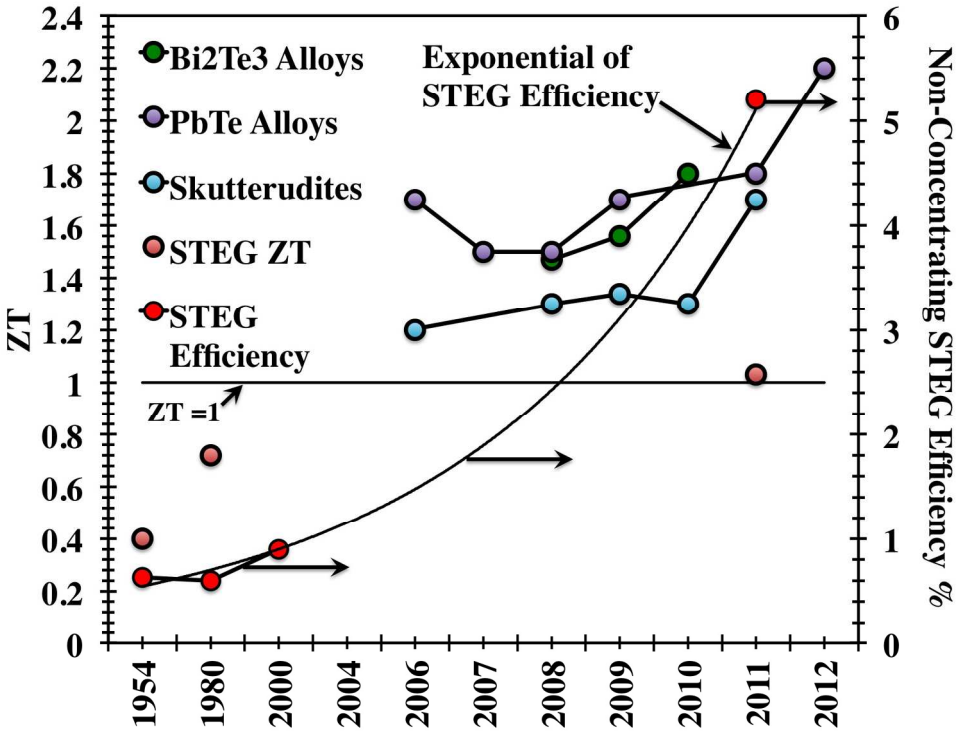

733x550mm (72 x 72 DPI)